2023-01-0224 Published 11 Apr 2023

A Synergic Use of Innovative Technologies for the Next Generation of High Efficiency Internal Combustion Engines for PHEVs: The PHOENICE Project

Toni TAHTOUH IFP Energies nouvelles I.Carnot IFPEN TE

Federico Millo, Luciano Rolando, and Giuseppe Castellano Politecnico di Torino

Mauro Brignone Marelli

Jason Cleeton Johnson Matthey ECT

Nicolas Demeilliers In Extenso Innovation Croissance

Gennaro Lucignano Stellantis

Juan Sierra Castellanos Garrett Motion

Alessandro Perazzo FEV Group GmbH

Citation: TAHTOUH, T., Millo, F., Rolando, L., Castellano, G. et al., "A Synergic Use of Innovative Technologies for the Next Generation of High Efficiency Internal Combustion Engines for PHEVs: The PHOENICE Project," SAE Technical Paper 2023-01-0224, 2023, doi:10.4271/2023-01-0224.

Received: 10 Nov 2022 Revised: 16 Jan 2023 Accepted: 29 Jan 2023

Abstract

Despite the legislation targets set by several governments of a full electrification of new light-duty vehicle fleets by 2035, the development of innovative, environmental-friendly Internal Combustion Engines (ICEs) is still crucial to be on track toward the complete decarbonization of on road-mobility of the future. In such a framework, the PHOENICE (PHev towards zerO EmissioNs & ultimate ICE efficiency) project aims at developing a C SUV-class plug-in hybrid (P0/P4) vehicle demonstrator capable to achieve a -10% fuel consumption reduction with respect to current EU6 vehicle while complying with upcoming EU7 pollutant emissions limits.

Such ambitious targets will require the optimization of the whole engine system, exploiting the possible synergies among the combustion, the aftertreatment and the exhaust waste heat recovery systems. Focusing on the first aspect, the combined use of innovative in-cylinder charge motion, Miller cycle with high compression ratio, lean mixture with cooled EGR and electrified turbocharger will enable a highly diluted combustion process capable to achieve a peak indicated efficiency of 47% and, at the same time, to minimize the engine out emissions. Numerical simulations were intensively exploited to reduce the engine calibration time and to preliminary assess the benefits of the abovementioned technologies. In particular, 3D-CFD simulations highlighted the capabilities of the Swumble^{TM} intake ports to produce an increase of about 50% of the Turbulent Kinetic Energy (TKE), while 1D-CFD models showed possible further enhancements of the brake thermal efficiency through the use of the new turbocharger (+2%) and of an aggressive Millerization of the cycle (+1.1%).

Finally, a preliminary experimental campaign, performed on the first engine prototype, confirmed the encouraging results of the simulation activity. With an AFR = 1.43 and an EGR ratio close to 5%, the PHOENICE engine showed a further improvement in the BTE up to 4% and a simultaneous reduction of the NOx emissions of more than 70% in comparison with conventional stoichiometric, undiluted operation.

Introduction

According to the European "Fit for 55" proposal, tank-to-wheel CO_2 emissions of passenger cars should be reduced by at least 55% by 2030 compared to 1990 levels [1]. In addition, upcoming Euro 7 legislation is expected to further decrease the limits for currently regulated air pollutant emissions as well as to introduce new ones for species that are not yet regulated, such as NH_3, N_2O, CH_2O and CH_4 [2]. To bridge the gap between laboratory testing and real driving conditions, it is also anticipated that conformity factors for Real Driving Emissions (RDE) compliance will be greatly reduced [3].

In such a context, hybrid electric powertrains are considered as the primary short-term solution to lower fuel consumption and exhaust emissions of Light-Duty Vehicles (LDVs). Theoretically, Plug-in Hybrid Electric Vehicles (PHEVs) can maximize the potential of both their electric and thermal powertrain components by extending their "zero emissions" range while driving in cities and attaining "near zero emissions" while driving on highways or in rural areas on longer trips. The high PHEVs flexibility presents a significant challenge because performance needs to be adjusted for all real-world scenarios while also taking unpredictable user charging and driving behaviour into account. Making the most of the hybrid architecture is therefore crucial.

There is general agreement that a significant portion of PHEVs on the market will have gasoline engines to keep customers' purchase costs as low as possible. The synergic use of a Spark-Ignition (SI) engine in conjunction with one or more electric machines enables the adoption of innovative technologies to boost the efficiency in the most frequently used operational area. Advanced Internal Combustion Engines (ICEs) fully adapted to hybrid powertrains could also reduce the demands on the battery size, resulting in a reduction in the cost of the vehicle. Finally, from the perspectives of air quality and regulation compliance, these high efficiency powertrains must also be combined with cutting-edge Exhaust After-Treatment Systems (EATS).

In this framework, the PHOENICE (PHev towards zerO EmissioNs & ultimate ICE efficiency) project seeks to create a C SUV-class plug-in hybrid vehicle demonstrator whose energy consumption and pollutant emissions will be simultaneously minimized for real-world driving scenarios, while maintaining acceptable vehicle performance and driveability [4]. Table 1 summarizes the overall targets of the project. In comparison with the baseline vehicle, the fuel consumption will be reduced by 10% on a Charge Sustaining (CS) WLTC driving cycle. The PHOENICE concept will also comply with the upcoming Euro 7 regulations and meet the emission levels outlined in the European Commission's Horizon Prize for the Cleanest Engine of the Future [5]. The optimization of newly developed ICE components, together with an improved after-treatment system and an additional waste heat recovery solution will take full use of numerical simulations. Thanks to this approach, the amount of prototype resources and development time can be decreased while maximizing the quality of the final integration on-board of the vehicle.

This paper will focus on preliminary results concerning engine development. Outcomes of extensive simulation campaign will be compared with the preliminary experimental measurements carried out on the first engine prototype.

TABLE 1 PHOENICE targets for (a) vehicle performance, (b) vehicle and engine efficiency, (c) pollutant emissions

Vehicle Performance Targets (*ICE+EM – **ICE Only)			
Max. Speed	165 km/h		
Acc. 0-100 km/h	10 s * – 13 s **		
Elasticity (60-100 km/h)	7 s * – 10 s **		
Gradeability	30 % * – 20 % **		
(a)			
Vehicle and Engine Efficiency Targets			
Fuel Consumption	-10% vs Baseline Vehicle (CS WLTC Test)		
ICE efficiency	47% Peak Indicated Eff.		
(b)			
Pollutants Emissions Ambitions (RDE)			
Regulated species		Unregulated species	
CO	400 mg/km	CH4	10 mg/km
NMOG	25 mg/km	HCOH	5 mg/km
NO_x	20 mg/km	N2O	10 mg/km
PM	1 mg/km	NH3	10 mg/km
PN (>10nm)	5×10^{10} #/km		
(c)			

PHOENICE Project Overview

Baseline Vehicle

The baseline for the PHOENICE demonstrator is a C SUV-class plug-in hybrid vehicle, shown in Figure 1. The hybrid architecture combines a latest generation gasoline engine, providing torque to the front axle via a 6-speed Automatic Transmission (AT) gearbox, with two electric motors placed in P0 and P4 positions. Figure 2 shows a schematic of the powertrain configuration. The e-motor in P4 position provides additional torque to the rear axle enabling the electric All-Wheel Drive (AWD) operation. Moreover, it acts as prime mover when the Electric Vehicle (EV) mode is selected. As a Belt-Starter Generator (BSG), the P0 combines the functions of conventional alternator and starter motor into a single device. It enables frequent S&S manoeuvres, and it is capable of energy harvesting from regenerative braking. As a result, both electric machines contribute to the energy recuperation during the vehicle braking phases.

FIGURE 1 PHEV C-SUV for PHOENICE demonstrator vehicle

FIGURE 2 Hybrid architecture of baseline vehicle

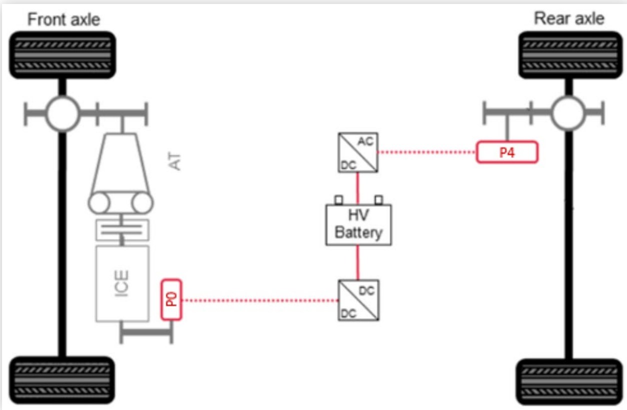

TABLE 2 Baseline vehicle specifications

Baseline Vehicle Specifications	
Curb weight	1935 kg
Max. Speed	200 km/h
Acc. 0-100 km/h	7.3 s
Fuel Consumption	2.1 L/100km (WLTP)
Battery SoC for CS mode	4.4%
CO_2 emissions	45 g/km (WLTP)
EV range	49 km (WLTP)
Emissions Standard	Euro 6d-final

Table 2 summarizes the baseline vehicle specifications. It should be remembered that, according to the European type-approval procedure [6], PHEVs are evaluated by means of the Worldwide Harmonized Light-Duty Vehicles Test Procedure (WLTP) in both Charge Depleting (CD) and Charge Sustaining modes. The type-approved fuel consumption is then obtained as the weighted average of the results from the two tests, computed according to the so-called Utility Factor (UF). The UF represents the percentage of time the car is operated in CD mode, which greatly depends on how frequently the user recharges the vehicle battery.

The baseline engine is a Stellantis 4-cylinder in-line turbocharged spark ignition engine with a displacement of 1.3 L [7]. It features all-aluminium structure with an integrated exhaust manifold in the cylinder head, long stroke design (Stroke/Bore = 1.24), compact 4-valves combustion chamber with high tumble inlet ports, high pressure side fuel injectors, and a MultiAir Variable Valve Actuation (VVA) system [8]. Together with those of the P4 e-Motor, engine performance in terms of peak power and torque are listed in Table 3.

PHOENICE Approach

The objective of the PHOENICE project is to demonstrate the full potential of a plug-in hybrid vehicle for reducing fuel consumption and pollutant emissions under real driving conditions. To achieve this goal, the demonstrator vehicle powertrain will be significantly revised in comparison with the baseline both on the engine and exhaust aftertreatment

TABLE 3 Hybrid powertrain parameters

Hybrid Powertrain Parameters		
ICE	Specs	1.3L 4-cyl in-line 16v
	Features	MultiAir VVA, GDI, TC with WG
	Bore × Stroke	70 × 86.5 mm
	Stroke/Bore	1.24
	Compression Ratio	10.5
	Max. Power	132 kW @ 5750 RPM
	Max. Torque	270 Nm @ 1850 RPM
	Transmission	6-speed AT
E-Motors	Location	P0 + P4
	Power (P4)	70/44 kW [peak/ continuous]
	Torque (P4)	250 Nm [peak]
HV Battery	Spec.	Li-Ion
	Capacity	11.4 kWh

sides. Furthermore, the energy management strategy will be optimized as well. The different areas of vehicle development are highlighted in Figure 3.

The introduction of different technologies for air charging and fuel injection on the baseline engine will enable a lean burn operation on a large portion of the engine map. The target is to reach an indicated peak efficiency of 47%. Additionally, the engine calibration will be oriented on making the most of the electrification potential. To be compatible with lean exhaust conditions, the exhaust after-treatment system will be upgraded with a Selective Catalytic Reduction (SCR) device. Furthermore, the Three-Way Catalyst (TWC) and the Gasoline Particulate Filter (GPF) performance will be enhanced to comply with the upcoming Euro 7 legislation limits. Finally, a Waste Heat Recovery System (WHRS) will be installed on the vehicle to further improve its overall energy efficiency. The engine, the after-treatment, and the waste heat recovery system will be controlled according to an

FIGURE 3 PHOENICE project development areas

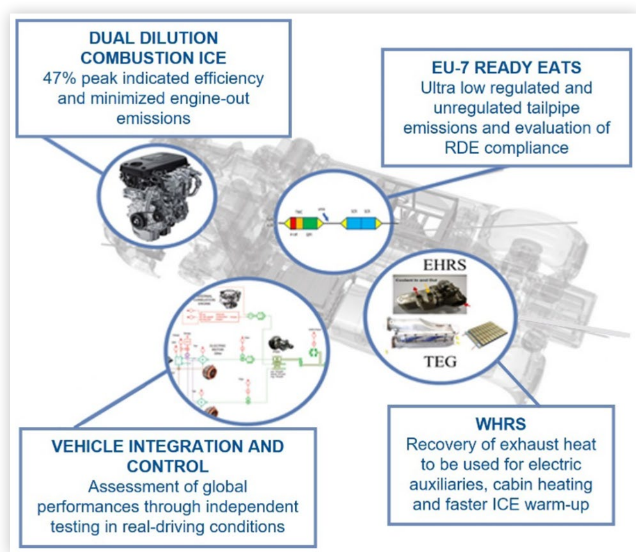

emission-based hybrid Energy Management Strategy (EMS). To reduce the amount of physical testing, the control strategy will first go through an extensive functional validation exploiting Hardware-In-the-Loop (HiL) methodology by means of FEV VCAP (Virtual Calibration Platform).

PHOENICE Engine Concept

Most of gasoline spark-ignition engines currently on the market are running with stoichiometric air/fuel mixtures. Due to their design and operating principle, these engines are usually limited to peak efficiencies of around 40%. Some recent engine concepts have achieved peak efficiencies of around 43% by combining high compression ratios with Exhaust Gas Recirculation (EGR) and improved tumble motion, together with optimized valve actuation strategies [9]. However, stoichiometric operation results in substantial pumping losses during the gas exchange process at low loads, high cooling losses due to the elevated combustion temperature, as well as significant energy losses at the exhaust. Pumping losses at low loads are less of an issue for PHEV applications since the EV mode can be chosen to prevent running the internal combustion engine in this region of extremely low efficiency. Nevertheless, in the areas of medium to high loads, losses due to heat transfer and to retarded combustion timings continue to be significant. To maximize PHEVs efficiency, it is then crucial to investigate novel approaches to engine design that could enable the minimization of all the aforementioned losses, especially in operating conditions where the vehicle cannot rely on electric propulsion and must unquestionably benefit from a highly efficient ICE. From this viewpoint, ultra-lean burn engines may be a viable solution to raise peak efficiency above 45% [10, 11]. The first benefit of high dilution is the large reduction in cooling losses because of the lower combustion temperature. For the same reason, diluting the air/fuel mixture improves knock resistance. Lean burn engines can therefore be designed with higher compression ratios than stoichiometric engines, which will enable them to reach a better thermodynamic efficiency. However, to support an ultra-lean combustion process, limiting as much as possible combustion instabilities, enhanced in-cylinder turbulence as well as sophisticated ignition and turbocharging technologies are needed [12].

In this framework, the PHOENICE engine concept, based on a state-of-the-art Stellantis 1.3 liter gasoline engine, will combine the benefits of air and EGR dilutions to achieve 47% of peak indicated efficiency and low engine-out emissions, while guaranteeing the required vehicle performance. Several innovative technologies, illustrated in Figure 4, have been taken into consideration for the engine design. The ultra-lean combustion approach will be supported by a high-pressure injection system up to 350 bar and a newly developed charge motion Swumble™ concept [13,14]. A new piston design will increase the compression ratio up to 13.6. Additionally, a 48V electrified turbocharging system [15] will be employed to supply the necessary boost pressure, as well as to recover waste enthalpy from exhaust gases when it is possible, and to

FIGURE 4 Highlights of new PHOENICE engine features

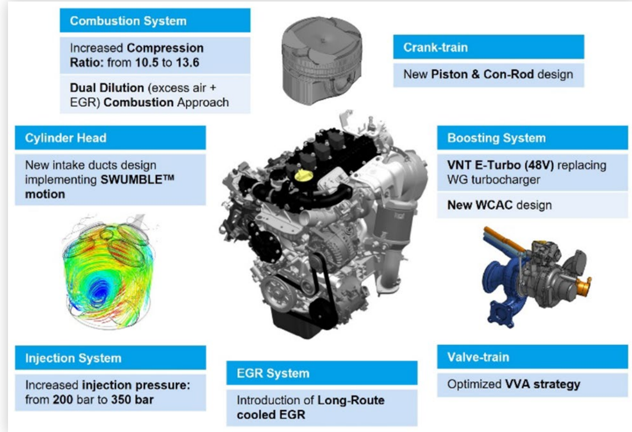

speed-up catalyst light-off following a cold-start. Finally, the fully variable MultiAir valve actuation system will also help to further increase thermodynamic efficiency by enabling Miller cycle exploitation [16, 17, 18], besides minimizing pumping losses at part load thanks to unthrottled operation [8].

The dual dilution strategy, exploiting lean mixture with EGR, in combination with Early Intake Valve Closing (EIVC) or Late Intake Valve Closing (LIVC) load control will reduce pumping losses thanks to de-throttling and minimize cooling losses as a result of lower combustion temperatures. Additionally, it will allow for more advantageous mixture characteristics in terms of heat capacity and polytrophic exponent, with further positive effects in terms of knock mitigation thanks to the introduction of EGR [19]. Indeed, the goal is to optimize the trade-off between efficiency and pollutant emissions across the whole engine map by using air and EGR as needed, based on the engine operating conditions. The primary dilution, air, seeks to greatly improve efficiency while reducing NOx and PN emissions. Limiting maximum EGR rates below 15%, EGR is viewed as a secondary dilution with a primary focus on strengthening the reduction of NOx emissions without significant efficiency disadvantages.

SWUMBLE™ In-Cylinder Motion

The IFPEN Swumble™ concept is an innovative approach to improve engine efficiency under a wide range of engine operating conditions. By redesigning the combustion chamber and the intake ducts, Swumble™ can enhance in-cylinder turbulent motion with just minor flow capacity degradation. Moreover, it is particularly well suited to early and late intake valve closing strategies with high dilution rates [13,14]. In this section, the integration and optimization of this feature on the base engine will be discussed and the resulting increase in turbulence intensity will be highlighted.

It is common knowledge that the charge motion within an internal combustion engine may be represented in terms of the three axes of reference (X, Y, and Z), as shown in Figure 5. The Swumble™ combines a high level of tumble motion around the Y axis with swirl motion around the Z axis.

FIGURE 5 Left: Axes of in-cylinder charge motion. Right: Swumble™ fluid motion as a combination of tumble (Y) and swirl (Z) motions

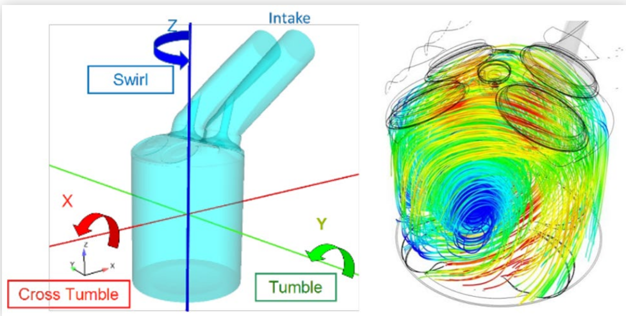

For an optimal application of the Swumble™ concept to the baseline cylinder geometry, a 3D-CFD flow simulation test bench was utilized to determine the impact of several geometrical modifications on the internal fluid dynamics. This test bench, simulating a motored engine, was in fact able to provide useful insights about the internal charge motion. Integral tumble and swirl ratios, as well as the average Turbulent Kinetic Energy (TKE) over the cylinder and the local value at spark plug, were used to rank the different design variants. To create a reference simulation, the geometries of the cylinder head, port, valves, and piston were obtained from a multicylinder CAD model of the baseline engine. In this study, the cylinder #2 was chosen and extracted from the multicylinder model. To account for the impact of the airbox on the flow structure, a portion of the plenum was included in the CFD simulations, as shown in Figure 6. Cylinder head, piston and intake ports design were thus selected for optimization.

The 3D-CFD motored engine test bench was operated at 2000 rpm, with constant 1 bar pressure at the domain boundaries on both intake and exhaust sides, and without taking into account injection nor combustion. Moreover, adiabatic conditions were imposed, with no heat transfer at the walls.

In the design optimization loops, two intake valve lift profiles were considered for each geometrical modification. The abovementioned valve lift profiles, illustrated in Figure 7, were extracted from the available Multi-Air system data. A Miller LIVC law was chosen with IVO ~360 CA @ 1mm lift and with a duration of ~231 CA. A Miller EIVC law with IVO ~360 CA @ 1mm lift and with a duration of ~138 CA was also considered.

RANS simulations were performed using commercially available 3D-CFD CONVERGE™ software, version 3.0.18 [20].

In addition to the flow motion, one of the objectives of the optimization process of the intake ports and of the combustion chamber geometry was to increase the compression ratio to around 13.6 to achieve higher thermodynamic efficiency. The re-designed piston geometry thus obtained is shown in Figure 8.

A comparison of the turbulence distribution in plane cuts centered on the spark plug for the baseline and for the optimized engine is shown in Figure 9. A globally higher

FIGURE 6 Computational model for the 3D CFD simulations

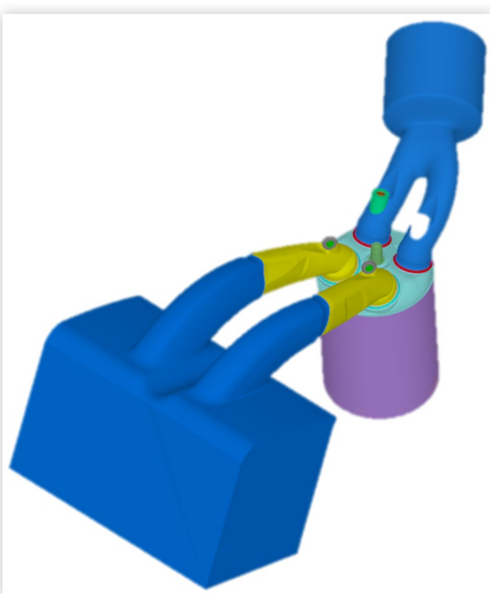

FIGURE 7 Selected valve lifts for CFD simulations

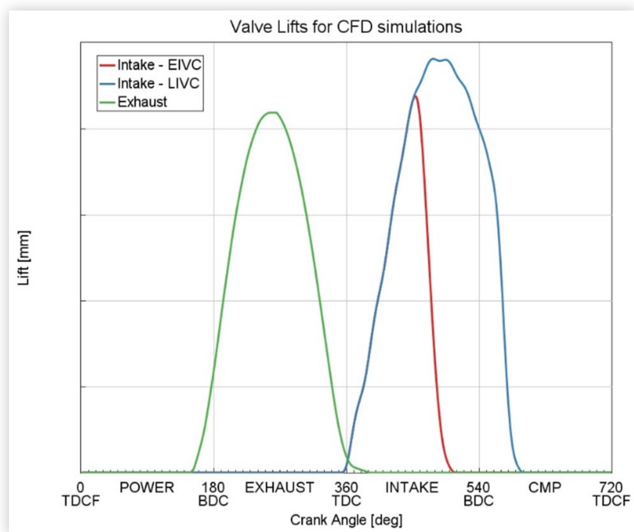

FIGURE 8 IFPEN new piston design with CR 13.6

FIGURE 9 Comparison of TKE distribution in planes aligned with the spark plug at TDC in LIVC configuration. Upper: reference engine. Lower: IFPEN optimization with CR 13.6

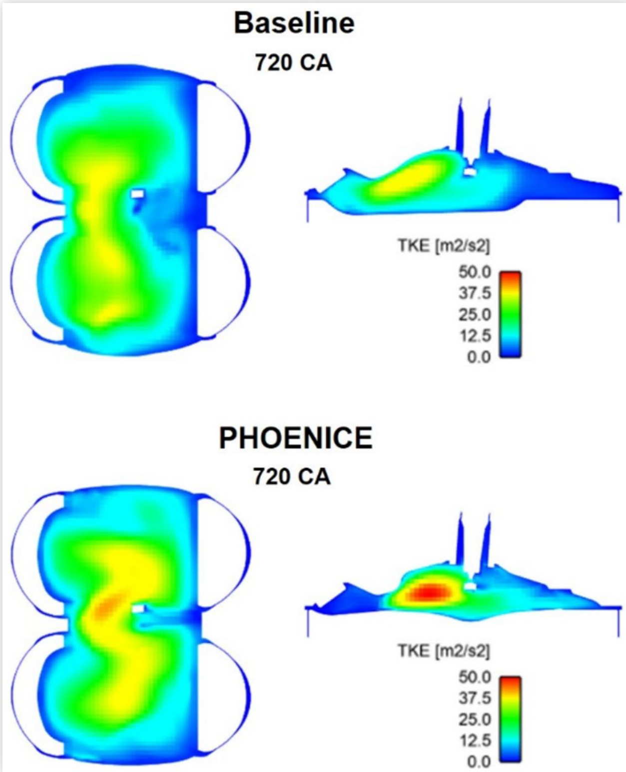

turbulence level after the design optimization was achieved, especially near the spark plug and on the exhaust side. Moreover, the turbulence is more evenly distributed in these planes after the optimization, which could be beneficial to the combustion process. It is important to remind that the injection was not simulated during this design phase. However, increased levels of turbulence are known to improve the quality of the mixture by achieving a more homogeneous fuel distribution in the combustion chamber.

Figure 10 provides some more insights on the increased turbulence motion for the two considered intake valve strategies, LIVC and EIVC. Numerical values in terms of TKE improvements are also reported in Table 4 The enhanced tumble flow motion converted into turbulence leads to a higher turbulence level on average in the cylinder, as well as locally at the spark plug. This relative increase in average TKE of about 50% for both valve strategies will contribute to a

TABLE 4 TKE improvements after Swumble^{TM} concept optimization. Comparison with baseline for Early and Late Miller configurations

TKE improvements in [%]	EIVC	LIVC
Average at 690 CA	+53%	+55.8%
Average at 700 CA	+54.4%	+49.7%
Average at 720 CA	+11%	+0.33%
@ Spark plug at 690 CA	+8.4%	+41.8%
@ Spark plug at 700 CA	+24.3%	+32.2%
@ Spark plug at 720 CA	+112%	+46.3%

FIGURE 10 Left: Tumble Ratio. Centre: average TKE in the cylinder. Right: TKE at the spark plug, averaged on a 5 mm box. EIVC and LIVC configurations

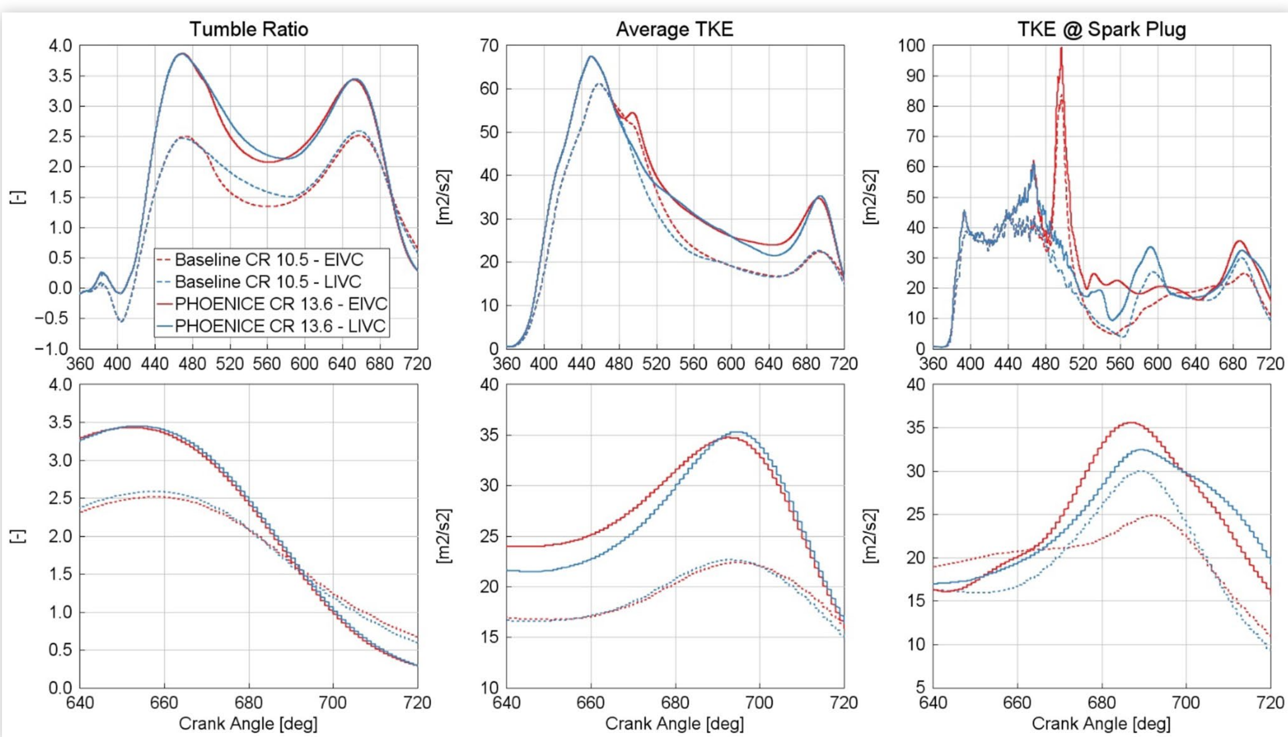

reduction in the combustion duration, therefore increasing engine efficiency.

E-Turbocharging

A new prototype of electric turbocharger has been specifically developed by Garrett for the PHOENICE project. It features a high temperature resistance Variable Nozzle Turbine (VNT) replacing the wastegate turbine of the baseline engine. Furthermore, a 48V e-Motor has been integrated on the turbo shaft, providing electrical assistance as well as power generation capabilities. The main parameters of this component can be found in Table 5.

The electrical assistance is fundamental not only to provide the necessary boosting pressure required by the extended lean engine operation, but also to improve the dynamic response during transient manoeuvres [21]. Moreover, the E-Turbo can be electrically operated right before engine start-up to significantly accelerate the electrically heated TWC warm-up. Finally, the exploitation of the excess exhaust energy by means of the electric machine used as a generator allows reducing the alternator load, thus offering additional fuel consumption reductions, which have been demonstrated to reach 2-3 % on WLTC [21].

Figure 11 shows a comparison between compressor and turbine maps of the baseline wastegate turbocharger and the PHOENICE VNT E-Turbo by Garrett. The optimized compressor has a higher pressure-ratio capability but a reduced mass flow capacity with respect to the baseline turbocharger. It features a much wider area of high efficiency, with the peak value that has been incremented by 4%. The optimized turbine vanes have been sized to obtain a similar characteristic to the baseline turbine when the VNT rack is 40% open.

The performance of the E-Turbo was evaluated exploiting the virtual test rig developed at Politecnico di Torino through the commercially available 1D-CFD code GT-Suite [22]. Two different PHOENICE engine model configurations were analyzed, with the baseline Waste-Gate (WG) turbo and the optimized VNT E-Turbo, respectively. Full load simulations in the acceptable performance scenario were run. This scenario implies limiting the engine torque and power to an acceptable level capable of ensuring the achievement of the vehicle performance target while simultaneously maximizing the efficiency. Stoichiometric operation was forced, avoiding any mixture enrichment for component protection. For both configurations, the same baseline engine intake valve lift profiles were applied. The different structural limits of the two turbochargers, in terms of maximum turbine inlet temperature and maximum turboshaft speed, were considered by the engine control logic. Finally, no electric boosting was provided. Figure 12 shows the simulated full load curve obtained with the Garrett VNT E-Turbo in comparison with the baseline WG turbo. The two BMEP profiles are quite close except for the deviation observed at 5000 RPM. The increase of BMEP level (+15%) obtained at this operating speed is consistent with the extended turbine inlet temperature (T3) limit of the optimized turbocharger.

From 2000 to 4000 RPM, both engine configurations reach the target BMEP. However, the optimized turbocharger leads to an improved Brake Thermal Efficiency (BTE) value of up to 2% at 4000 RPM. Figure 13 shows compressor efficiency together with turbine inlet pressure for the two datasets under discussion. Thanks to the higher compressor efficiency, the required boost can be achieved with reduced exhaust backpressure by opening more the turbine vanes of the E-Turbo.

This results in lower residuals content, with an improved knock resistance, leading to better combustion phasing, as it can be seen in Figure 14. The crossover observed at 5000 RPM

TABLE 5 Garrett E-Turbo Operating Parameters

Garrett E-Turbo Operating Parameters	
Boost Control	Variable Nozzle Turbine
Max. Compressor Outlet P	4 bar
Max. Turbine Inlet T	1020 °C
System Voltage	48 V
eMotor Continuous Rating	2.5 kW

FIGURE 11 Compressor and turbine maps comparison

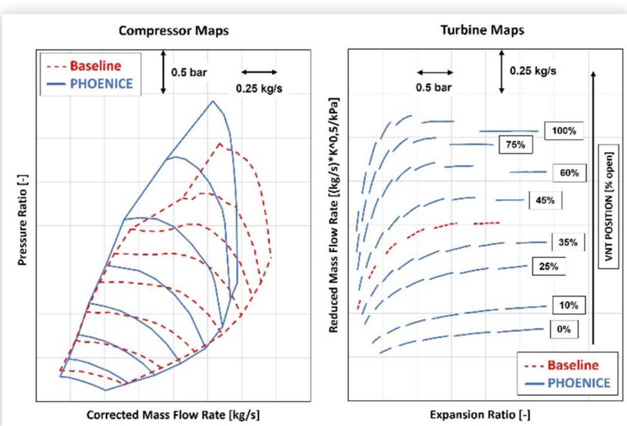

FIGURE 12 Full Load Curves comparison between baseline WG turbo and Garrett VNT E-Turbo: BMEP and BTE

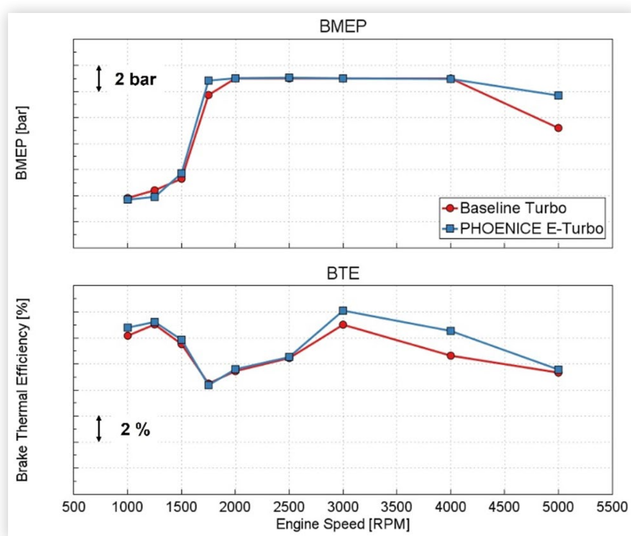

FIGURE 13 Full Load Curves comparison between baseline WG turbo and Garrett VNT E-Turbo: Compressor Efficiency and Turbine Inlet Pressure

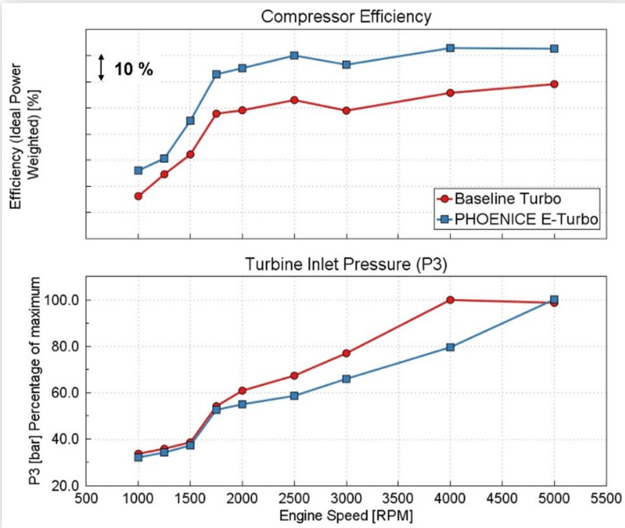

FIGURE 14 Full Load Curves comparison between baseline WG turbo and Garrett VNT E-Turbo: MFB50 and PMEP

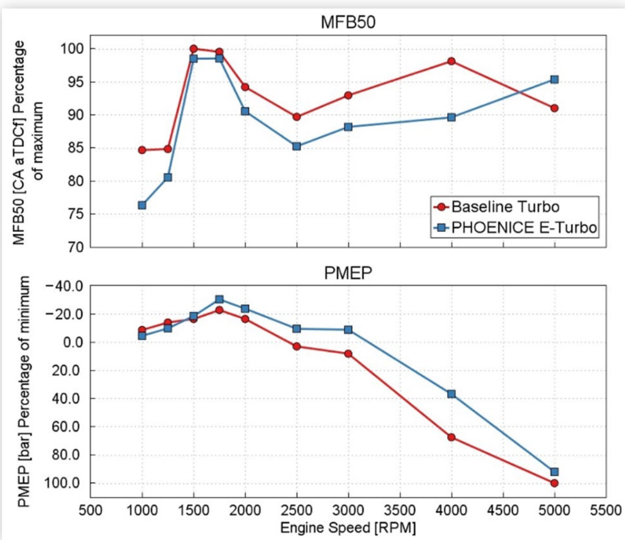

is a consequence of the T3-limited operation of the baseline turbo configuration. At this speed point, the engine controller must open further the wastegate at the expense of a reduced boost pressure. Lower boost implies a lower tendency to knock, which leads to better phased combustion. Moreover, pumping losses are reduced as well, further improving the efficiency with respect to the baseline.

Aftertreatment System

The PHOENICE engine is anticipated to mostly work in lean conditions with frequent stop-start events. The challenge is therefore to achieve a high emissions conversion efficiency in these conditions. The most effective option to achieve lean

TABLE 6 Comparison between baseline and PHOENICE EATS components dimensions

Component	Baseline Vol. [L]	PHOENICE Vol. [L]
EHC-TWC (CC)	0.82	1.5
GPF (CC)	1.4	2.5
NO-Ox (UF)	N/A	1
SCR (UF)	N/A	2.5
ASC (UF)	N/A	2.5

NOx conversion is to exploit SCR technology. Unlike in conventional diesel system, SCR will need to tolerate stoichiometric/rich conditions and high temperatures at full load. Furthermore, a three-way catalyst with an excellent conversion efficiency for HC, CO and NOx under stoichiometric operating conditions and a good oxidation capability for HC and CO under lean conditions, has to be combined with the previously mentioned SCR system. Filtration of particles down to 10 nm-size without excessive backpressure is necessary. Consequently, TWC and GPF bricks were updated both in geometry and formulation. Table 6 shows a comparison between baseline and PHOENICE after-treatment system, in terms of components volume.

Finally, improved thermal management thanks to electrical heating, has been obtained to ensure low cold start and stop-start emissions. Through an iterative process, the system has been reviewed and optimized and a final after-treatment system layout for the demonstrator vehicle, shown in Figure 15, has been identified by Johnson Matthey.

Exhaust Waste Heat Recovery System

As far as the WHRS is concerned, PHOENICE will focus on Exhaust Gas-to-Coolant Heat Recovery System (EHRS) and on Thermo-Electric Generator (TEG) devices, with the aim of finding the best trade-off between increased vehicle overall efficiency and cost. EHRS can be employed for smart cabin heating strategy and engine warm-up. TEG can provide additional power to the vehicle electrical network. A suitable combination of the two technologies might also be the final solution for hybrid powertrains, providing both increased electric energy and heat to be used for electric auxiliaries and for cabin or engine faster warm-up. A passive system is preferable to reduce costs, but an active controlled by-pass system can provide benefits in terms of overall recovered energy. A heat exchange efficiency greater than 80% is expected. The most suitable system for the improvement of real-world fuel consumption and the reduction of particle emissions will be installed and tested on the demonstrator vehicle.

FIGURE 15 PHOENICE EATS layout

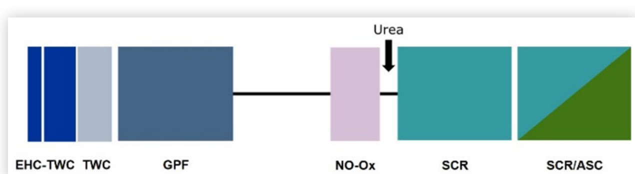

Preliminary Engine Calibration

As shown in Figure 16, the first engine prototype has been assembled and installed at the IFPEN test bench. Most of the new features, including the high-pressure injection system, the long-route EGR loop, and the rebuilt airline embedding the new Water-Charge Air Cooler (WCAC), have been successfully implemented. On the other hand, the baseline turbocharger and exhaust aftertreatment system were used for the initial tests.

To validate the new functionalities and begin the first steady state engine calibration, six representative operating points were identified, as reported in Table 7. Additionally, a second engine prototype has been built for the following transient calibration which will be carried out at Politecnico di Torino test facilities.

Numerical simulations have been used extensively in these early stages. To support the physical testing program, Politecnico di Torino conducted a preliminary assessment of the capabilities of the new lean combustion system and of its sensitivity to engine actuations by means of 1D-CFD GT-Suite simulations. First, the baseline engine model provided by Stellantis was upgraded to incorporate all the PHOENICE new features. This virtual test rig benefited from predictive combustion and knock models which were previously calibrated for the baseline engine [23] due to the lack of experimental data during the earliest phases of the PHOENICE project.

An example of how the numerical simulation has been exploited to support the new engine design and calibration is reported in the following section, where the results of a first sensitivity analysis on intake valves actuation in stoichiometric conditions without EGR and of a preliminary assessment of dual dilution combustion for the 3000 RPM, 7 bar BMEP operating condition will be discussed and compared with the results of the experimental tests.

FIGURE 16 PHOENICE engine prototype at IFPEN test facilities

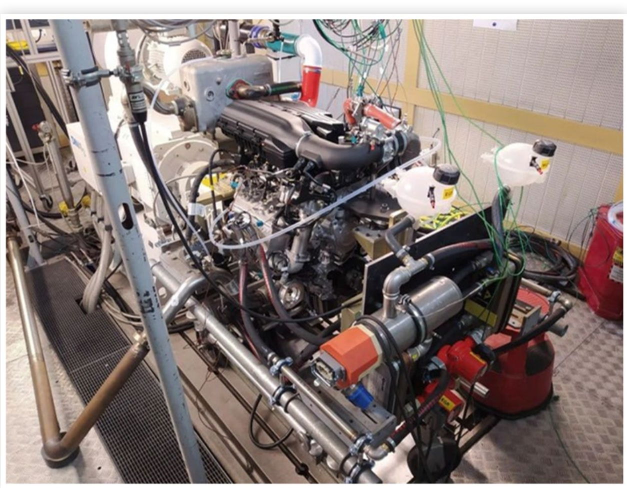

TABLE 7 Engine operating points for preliminary steady-state calibration

Key Point ID	ICE Speed [RPM] × BMEP [bar]
1	1500 × 2
2	1500 × 5.5
3	2000 × 13.5
4	2600 × 15
5	3000 × 7
6	3000 × 13

Valve Phasing Optimization

The PHOENICE engine benefits from fully variable valve actuation technology: the MultiAir electro-hydraulic actuation system allows complete control over the timing and the lift profile of the intake valves. As an example, Figure 17 illustrates MultiAir capability in terms of possible intake valve lift profiles at 3000 RPM with electric IVO (eIVO) set at 345 CA aTDCf.

To find the best combination of IVO and IVC capable of minimizing the Brake Specific Fuel Consumption (BSFC), a sensitivity analysis on the intake valve phasing was performed for the six representative operating points identified on the engine map. The ultimate goal was to assess the benefits of Early and Late Miller cycles [16]. For this first preliminary investigation, stoichiometric conditions without EGR were considered. Both the physical engine test bench and the virtual test rig were used to conduct the activity simultaneously. The eIVO range under consideration spanned from 305 to 395 CA aTDCf. Instead, the eIVC was adjusted from 480 to 680 CA aTDCf. Figure 18 displays the results of the simulation for one of the chosen operating conditions, 3000 RPM and 7 bar BMEP, in terms of BTE, combustion phasing (MFB50), and pumping losses (PMEP). The highest BTE points for the two proposed valve strategies are highlighted on the BTE plot with markers.

FIGURE 17 MultiAir intake valve lift profiles at 3000 RPM for eIVO = 345 CA aTDCf

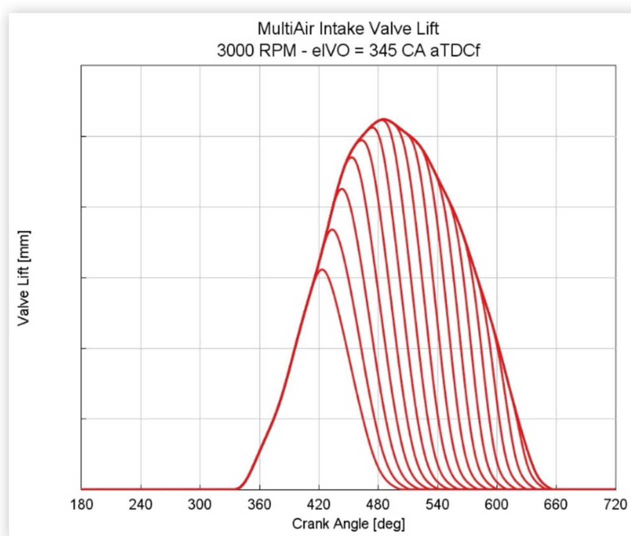

FIGURE 18 3000 RPM × 7 bar BMEP. Valve phasing optimization. Simulation results: BTE, combustion phasing and pumping losses

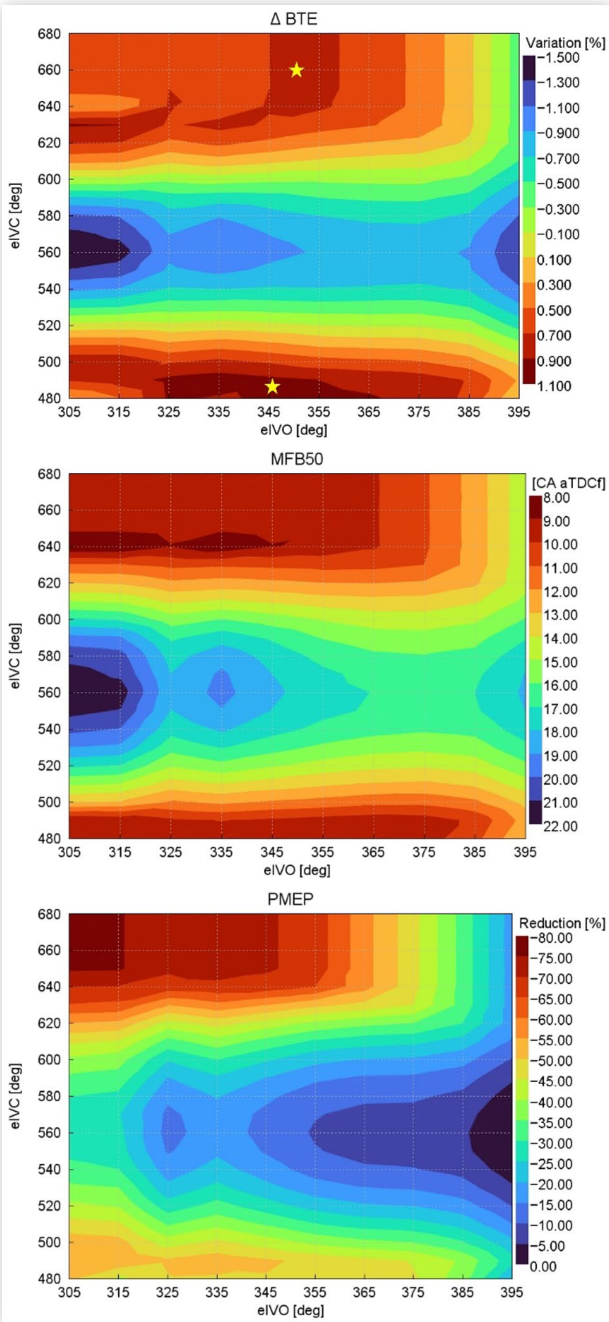

Evidence from simulation demonstrated that both EIVC and LIVC valve phasing led to improved efficiency, with increases in BTE of up to 1% over baseline engine value. This happens for EIVC values close to 490 CA aTDCf and for LIVC values between 640 to 680 CA aTDCf respectively. In fact, by moving the MFB50 closer to the optimal value of 8 CA aTDCf, the decreased in-cylinder pressure and temperature during spark ignition led to a better phased combustion process. This is a direct consequence of the decoupling between compression and expansion strokes. In addition, significant de-throttling is observed thanks to the highly anticipated or retarded

FIGURE 19 3000 RPM × 7 bar BMEP. Valve phasing optimization. Experimental results: BTE improvements

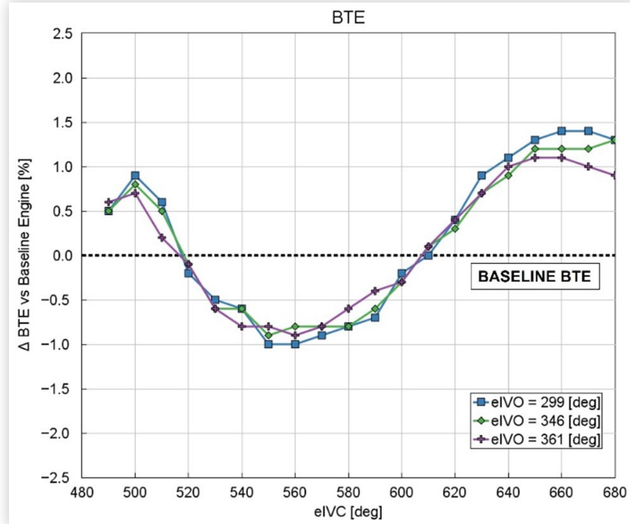

intake valve closing. This greatly reduces pumping losses, which are minimized in the case of LIVC, and thus raises engine efficiency even further. On the other hand, for early eIVO, a zone of delayed combustion can be found for eIVC around 560 CA aTDCf. This is because of the large amount of residuals left over from early opening of the intake valve lift profile.

Figure 19 illustrates the experimental results under stoichiometric conditions and without EGR in terms of BTE variation compared to baseline engine for the same intake valve actuation sensitivity analysis which was experimentally performed at the IFPEN test bench. The correlation between simulation and experimental testing results is more than satisfactory. Both numerical and experimental findings provide consistent estimates of the BTE increases which can be obtained by means of both Early and Late Intake Valve Closures. However, on the experimental side, Late Miller proved to be the best option to maximize BTE, providing higher efficiency benefits in comparison with Early Miller thus confirming previous results reported in literature [17]. On the other hand, for all the considered eIVO, the worst values were found in an area of IVC near to 560 CA aTDCf.

This initial investigation of valve phasing produced some very encouraging outcomes since a considerable increase in efficiency could be attained even in stoichiometric conditions without EGR. This highlights the advantages due to the enhanced Swumble™ in-cylinder motion as well as the increased compression ratio.

Dual Dilution Combustion Assessment

Dual Dilution combustion was preliminary assessed by means of a test campaign at engine bench involving an EGR sweep for different AFR spanning from stoichiometric conditions up to lean operation at lambda 1.43. For each of the test points, the valve phasing was left fixed. Figure 20 and Figure 21

FIGURE 20 3000 RPM × 7 bar BMEP. EGR sweep for different Air-Fuel Ratios. Experimental results: BTE improvements and CoV of IMEP

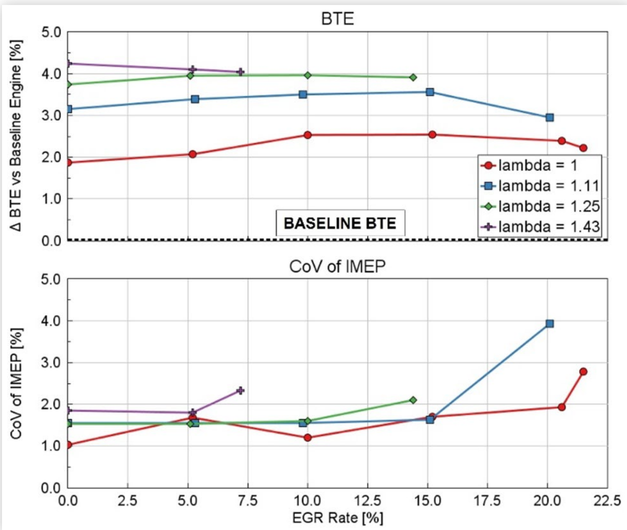

FIGURE 21 3000 RPM × 7 bar BMEP. EGR sweep for different Air-Fuel Ratios. Experimental results: CO, HC and NOx engine-out emissions

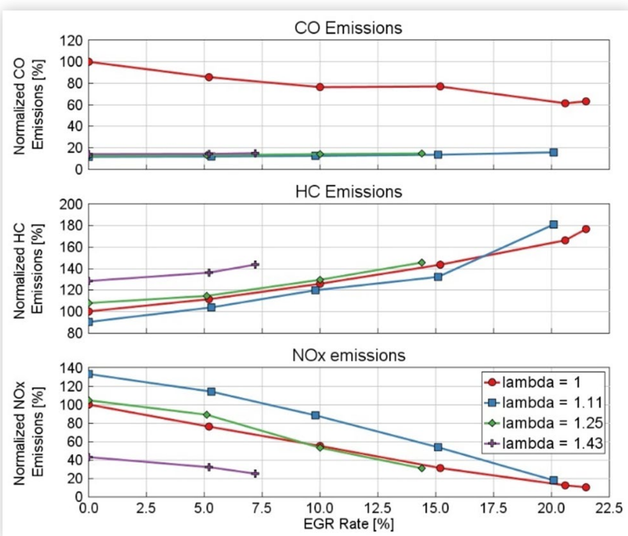

summarize the outcomes in terms of BTE improvements, Coefficient of Variation (CoV) of IMEP and engine-out pollutant emissions for the same operating condition considered in the previous section. As anticipated, air dilution significantly increases engine efficiency. Indeed, a better phased combustion can be achieved with more advanced spark timing thanks to dilution ability to improve knock resistance. Furthermore, heat losses are decreased because of the lower combustion temperature. Finally, the higher air flow rate needed to maintain lean operation results in an increase in boost pressure and in a more open throttle valve, which lowers pumping losses. When lambda is at 1.43, the leanest condition, the BTE figures differ by more than 4% from the baseline engine. Whereas EGR fraction has little impact on BTE, it has a significant impact on NOx emissions. As the EGR rate increases, NOx emissions show a dramatic decrease and can be readily cut by more than 80% for EGR rates greater than 15%, without any significant deterioration of combustion stability or CO emissions. On the contrary, higher EGR rates cause more unburned hydrocarbon emissions, however the reduction in NOx outweighs the penalty on HC.

Conclusions

In this paper, preliminary results achieved to date from the PHOENICE project were presented. A new lean-burn spark ignition engine concept was developed based on a state-of-the-art Stellantis 1.3 liter gasoline engine. A number of innovative technologies were selected to maximize the synergy with the hybrid architecture of the PHEV demonstrator vehicle. Swumble™ in-cylinder charge motion was exploited to enable dual-dilution combustion approach, that utilizes excess air and EGR. To this extent, 3D-CFD simulations were performed to optimize the intake ports geometries and piston design and to evaluate the benefits of this innovative technology in terms of turbulent motion enhancement. Moreover, a new charging system featuring an electrically assisted turbocharger allows the engine to operate with high dilution levels and enables strong EIVC and LIVC Miller strategies. A new EATS with diesel-like SCR and EHC was developed and optimized for engine lean operation. Initial testing on the first engine prototype yielded some very encouraging findings. The effectiveness of the dual dilution combustion was assessed for an engine operating point at 3000 RPM and 7 bar BMEP. For the leanest AFR operation with an EGR ratio close to 5%, improvements in brake thermal efficiency up to 4% and reductions in NOx emissions more than 70% were achieved, in comparison with conventional stoichiometric, undiluted operation.

Future work will be focused on further optimization of engine calibration exploiting both numerical simulation and physical testing, under both steady state and transient operating conditions. The benefits of the new approach in terms of virtual calibration methods will be evaluated against the conventional state-of-the-art approaches. Starting in the first quarter of 2024, a vehicle demonstrator will be available for the final assessment of the project objectives.

References

1. Ovaere, M. and Proost, S., "Cost-Effective Reduction of Fossil Energy Use in the European Transport Sector: An Assessment of the Fit for 55 Package," *Energy Policy* 168 (2022): 113085, doi:https://doi.org/10.1016/j.enpol.2022.113085.
2. Samaras, Z., Kontses, A., Dimaratos, A., Kontses, D. et al., "A European Regulatory Perspective towards a Euro 7 Proposal," SAE Technical Paper 2022-37-0032, 2022, https://doi.org/10.4271/2022-37-0032.

3. Claßen, J., Krysmon, S., Dorscheidt, F., Sterlepper, S. et al., "Real Driving Emission Calibration—Review of Current Validation Methods against the Background of Future Emission Legislation," *Applied Sciences (Switzerland)* 11, no. 12 (2021), doi:https://doi.org/10.3390/app11125429.
4. PHOENICE Project Website, accessed November 9, 2022, https://phoenice.eu/.
5. EU Horizon2020 Website, accessed November 9, 2022, https://research-and-innovation.ec.europa.eu/funding/funding-opportunities/prizes/horizon-prizes_en.
6. "Commission Regulation (EU) 2017/1151 of 1 June 2017 supplementing Regulation (EC) No 715/2007 of the European Parliament and of the Council," accessed November 9, 2022, https://eur-lex.europa.eu/eli/reg/2017/1151/2020-01-25.
7. De Marino, C., Maiorana, G., Pallotti, P., Quinto, S. et al., "The Global Small Engine 3 and 4 Cylinder Turbo: The New FCA's Family of Small High-Tech Gasoline Engines," in *39th International Vienna Motor Symposium*, Vienna, April 26-27, 2018.
8. Bernard, L., Ferrari, A., Micelli, D., Peretto, A. et al., "Electro-hydraulic Valve Control with MultiAir Technology," *MTZ Worldw* 70 (2009): 4-10, doi:https://doi.org/10.1007/BF03226988.
9. Yang, D., Lu, G., Gong, Z., Qiu, A. et al., "Development of 43% Brake Thermal Efficiency Gasoline Engine for BYD DM-i Plug-in Hybrid," SAE Technical Paper 2021-01-1241, 2021, https://doi.org/10.4271/2021-01-1241.
10. Osborne, R., Lane, A., Turner, N., Geddes, J. et al., "A New Generation Lean Gasoline Engine for Premium Vehicle CO_2 Reduction," SAE Technical Paper 2021-01-0637, 2021, https://doi.org/10.4271/2021-01-0637.
11. Bunce, M., Peters, N., Pothuraju Subramanyam, S., Blaxill, H. et al., "The Impact of Advanced Fuels and Lubricants on Thermal Efficiency in a Highly Dilute Engine," *SAE Int. J. Adv. & Curr. Prac. in Mobility* 3, no. 5 (2021): 2540-2553, doi:https://doi.org/10.4271/2021-01-0462.
12. Scarcelli, R., Matthias, N., and Wallner, T., "Numerical Investigation of Combustion in a Lean Burn Gasoline Engine," SAE Technical Paper 2013-24-0029, 2013, https://doi.org/10.4271/2013-24-0029.
13. Bourhis, G., Laget, O., Kumar, R., and Gautrot, X., "Swumble In-Cylinder Fluid Motion: a Pathway to High Efficiency Gasoline SI Engines," in in *27th Aachen Colloquium Automobile and Engine Technology*, Aachen, October 8-10, 2018.
14. Gautrot, X., Bardi, M., Leroy, T., Luca, P. et al., "Swumble™ In-Cylinder Fluid Motion for High Efficiency Gasoline SI Engines: Development of the Second Generation," in *Proceedings of the SIA Powertrain and Electronics*, Rouen, November 16-29, 2020.
15. Davies, P., Bontemps, N., Tietze, T., and Faulseit, E., "Electric Turbocharging - Key Technology for Hybridized Powertrains," *MTZ Worldw* 80 (2019): 30-37, doi:https://doi.org/10.1007/s38313-019-0096-y.
16. Li, T., Gao, Y., Wang, J., and Chen, Z., "The Miller Cycle Effects on Improvement of Fuel Economy in a Highly Boosted, High Compression Ratio, Direct-Injection Gasoline Engine: EIVC vs. LIVC," *Energy Convers Manage* 79 (2014): 59-65, doi:https://doi.org/10.1016/j.enconman.2013.12.022.
17. Luisi, S., Doria, V., Stroppiana, A., Millo, F. et al., "Experimental Investigation on Early and Late Intake Valve Closures for Knock Mitigation through Miller Cycle in a Downsized Turbocharged Engine," SAE Technical Paper 2015-01-0760, 2015, https://doi.org/10.4271/2015-01-0760.
18. Millo, F., Luisi, S., Borean, F., and Stroppiana, A., "Numerical and Experimental Investigation on Combustion Characteristics of a Spark Ignition Engine with an Early Intake Valve Closing Load Control," *Fuel* 121 (2014): 298-310, doi:https://doi.org/10.1016/j.fuel.2013.12.047.
19. Tornatore, C., Bozza, F., Bellis, V. de, Teodosio, L., Valentino, G., and Marchitto, L., "Experimental and Numerical Study on the Influence of Cooled EGR on Knock Tendency, Performance and Emissions of a Downsized Spark-Ignition Engine," *Energy* 172:968-976, 2019, https://doi.org/10.1016/j.energy.2019.02.031.
20. Richards, K.J., Senecal, P.K., and Pomraning, E., *Converge 3.0 Manual* (Madison, WI: Convergent Science Inc., 2020)
21. Cooper, A., Bassett, M., Hall, J., Harrington, A. et al., "HyPACE - Hybrid Petrol Advance Combustion Engine - Advanced Boosting System for Extended Stoichiometric Operation and Improved Dynamic Response," SAE Technical Paper 2019-01-0325, 2019, https://doi.org/10.4271/2019-01-0325.
22. *GT-SUITE Engine Performance Application Manual, Software User Manual* (Westmont, IL, USA: Gamma Technologies, 2022)
23. Millo, F., Gullino, F., and Rolando, L., "Methodological Approach for 1D Simulation of Port Water Injection for Knock Mitigation in a Turbocharged DISI Engine," *Energies (Basel)* 13, no. 17 https://doi.org/10.3390/en13174297.

Contact Information

Dr. Toni Tahtouh
IFP Energies Nouvelles - Mobility and Systems Division
1 et 4 avenue de Bois-Préau
92852 Rueil-Malmaison Cedex – France
toni.tahtouh@ifpen.fr

Acknowledgments

This project has received funding form the European Union's Horizon 2020 research and innovation programme under Grant Agreement No. 101006841

Definitions/Abbreviations

1D-CFD - One-Dimensional Computational Fluid-Dynamics

3D-CFD - Three-dimensional Computational Fluid-Dynamics

AFR - Air-to-Fuel Ratio

ASC - Ammonia Slip Catalyst

aTDCf - After Top Dead Centre of Firing
AWD - All Wheel Drive
BMEP - Brake Mean Effective Pressure
BSFC - Brake Specific Fuel Consumption
BSG - Belt-Starter Generator
BTE - Brake Thermal Efficiency
CA - Crank Angle Degree
CAD - Computer-Aided Design
CC - Close Coupled
CD - Charge Depleting
CoV - Coefficient of Variation
CR - Compression Ratio
CS - Charge Sustaining
C-SUV - Segment C Sport Utility Vehicle
EATS - Exhaust After-Treatment System
EGR - Exhaust Gas Recirculation
EHRS - Exhaust Gas to Coolant Heat Recovery System
EIVC - Early Intake Valve Closing
EMS - Energy Management Strategy
EV - Electric Vehicle
GDI - Gasoline Direct Injection
GPF - Gasoline Particulate Filter
HiL - Hardware-In-the-Loop
ICE - Internal Combustion Engine
LDV - Light-Duty Vehicle
LIVC - Late Intake Valve Closing
MFB50 - Mass Fraction Burned 50% Crank Angle
NEDC - New European Driving Cycle
PHEV - Plug-in Hybrid Electric Vehicle
PHOENICE - PHev towards zerO EmissioNs & ultimate ICE efficiency
PMEP - Pumping Mean Effective Pressure
PMEP - Pumping Mean Effective Pressure
PN - Particle Number
RANS - Reynolds Averaged Navier-Stokes
RDE - Real Driving Emissions
SCR - Selective Catalytic Reduction Catalyst
SI - Spark Ignition
TEG - Thermo-Electric Generator
TKE - Turbulent Kinetic Energy
TWC - Three-Way Catalytic Converter
UF - Utility Factor
VNT - Variable Nozzle Turbine
VVA - Variable Valve Actuation
WCAC - Water-Charge Air Cooler
WG - Waste Gate
WHRS - Waste Heat Recovery System
WLTC - Worldwide Harmonized Light Duty Vehicles Test Cycle
WLTP - Worldwide Harmonized Light Duty Vehicles Test Procedure

ISSN 0148-7191